Bulgarian Chemical Communications, Volume 50, Special Issue L (pp. 310– 318) 2018

Investigation of kinetics and mechanism of the sulfating roasting process of chalcopyrite concentrate for water-leaching

Shahram Daneshpajooh*, Mohammadreza Mozdianfard

Department of Chemical Engineering, Engineering Faculty, University of Kashan, Kashan, Iran

Received February 25 2018, Revised April 09 2018

The kinetics of sulfate roasting process of chalcopyrite concentrate was investigated in the absence of mass transfer effects in the temperature range 500 to 625 ° C. From the study of mechanism of the sulfate roasting process by thermal analysis of TG-DSC and XRD analysis, it was observed that the production of copper sulfate starts at a temperature of about 500 ˚C and extends to a temperature of about 580 ˚C. Subsequently, as the temperature rises, the copper sulfate is converted to copper oxide. After the roasting tests, it was first shown that the kinetics controller of the process inside the chalcopyrite particle is the reaction at the level of the raw materials and products, and the penetration factor is less effective. The activation energy of the chalcopyrite sulfating reaction was 20.818 kJ/mol based on the unreacted core kinetic model.

Keywords: Chalcopyrite, Sulfate roasting, Kinetics, Mechanism, TG-DSC, XRD

INTRODUCTION

Numerous processes have been proposed and used so far for the oxidation of chalcopyrite and copper recovery [1]. Sulfate roasting is one of the important techniques that can be taken to recover copper from its sulfides. The purpose of the sulfate roasting process is to produce water-soluble copper sulfate, and insoluble iron oxide to solve the iron control problem [2], which is appropriate regarding cost and final product and environmental factors. Sulfate roasting is performed to convert copper sulfide to water-soluble copper sulfate and also iron sulfides to insoluble iron oxide [3]. This process was investigated using a fluidized bed micro-reactor at a temperature range of 200 to 700 °C [4]. At 555 ° C, the best temperature was obtained to produce the highest amount of copper sulfate. The researchers also experimented the recovery of zinc and copper from concentrate by using the fluidized bed and fixed bed furnaces [5]. The products of the furnaces were placed under leaching process at different concentrations of acid and temperatures. The maximum copper recovery was 65% in leaching with water. In another study, sulfate roasting tests were performed on a multi-metal concentrate containing 1.25% copper [6]. In these experiments, a porcelain aluminum tubular furnace was used. The largest amount of copper recovery for leaching in water which was equal to 65%, was carried out at a temperature of 550 ° C. Also, the energy needed to carry out the process was obtained.

Knowing the mechanism and oxidation velocity of the sulfate roasting process is important to ensure that the desired phases are obtained as the ultimate products and the feasible kinetics achieve industrially [7]. Some research showed that the formation of bornite was first and followed by the formation of magnetite [8-11]. According to Razuk et al. [12], at temperatures below 673K covellite form and then decompose into sulfate and oxide. At higher temperatures, copper sulfate is obtained from the interaction between CuO and Fe2(SO4)3. Higher than 873 K, copper sulfate and iron sulfate are both decomposed. The obtained oxides are reacted, and formed ferrite above a temperature of 1173K. Leung et al. concluded that oxidation occurs in the process of roasting through two way: direct oxidation of chalcopyrite to Fe3O4 and pyrrhotite oxidation resulted from chalcopyrite decomposition [8].

Various models were used for the study of kinetic of the chalcopyrite roasting process. Mitovsky [13] obtained the activation energy of copper multi-metal concentrate oxidation, which included chalcopyrite, enargite and pyrite, equal to 124 kJ/mol using the half-time model. Chaubal and Sohn examined the activation energy of the process in the presence of air. According to their studies, the kinetics of the roasting process at temperatures below 873K follows the pore blocking model, and above it conforms to the power law model. The activation energy was obtained to 71 kJ/mol using a pore blocking model at a temperature below 873K, and it calculated to 70 kJ/mol in the range of temperatures between 873 and 1030 K by using the power law model.

Ganguly et al. examined the mechanism and kinetics of the copper sulfide oxidation process

* To whom all correspondence should be sent:
E-mail: daneshpajouh2005@yahoo.com

using a tubular furnace [14]. Finally, by examining the experimental data and comparing the models, the "nucleation with branching and overlapping" model was selected with a correction factor of 0.95. Ramakrishna investigated the kinetics of roasting process on copper sulfide (Cu2O) pellet [15]. In this study, the unreacted core kinetic model was used for the solid-gas reaction. Prasad also studied the kinetics of chalcopyrite sulfate roasting process using the gas flow of oxygen and steam both in the presence and absence of ferric oxide (Fe2O3) [16]. In this research, unreacted core kinetic model was used to obtain activation energy of reactions. The results showed that the activation energy of the reaction decreases with the use of 10 wt% of ferric oxide in the solid sample.

MATERIALS AND METHOD OF RESEARCH

In this research, chalcopyrite concentrates of Sarcheshmeh copper mine (Iran) were used with the compounds presented in Tables 1 and 2. Chemical elements of the concentrate were determined by XRF analysis and mineralogy using an optical microscope. The device XRFPW1480 model from Philips Company was used for the XRF analysis.

The phase evaluation in the powders and the structural features of the samples before and after roasting was investigated using X-ray diffraction method (XRD, Philips X'pert) using Cu K_radiation working with 30 kV accelerating voltage, a [illegible]mA current and 0.5◦/sec.

For thermal analysis and determination of the processing mechanism, the concentrate sample were placed under atmospheric air and the temperature increases by a rate of 5, 10 and 20 °C/min, at a temperature range of 25 to 800 °C. The TG-DSC analysis was performed by the STA device PC Luxx 409 model from NETZSCH Co. manufactured in Germany.

Roasting tests were performed under atmospheric conditions. Lenton tubular furnace made in England was used for the purpose of conducting the tests.

To investigate the process of sulfate dissolution and its recovery rate, all leaching experiments were carried out at 70 ° C, 10% w / v (200 ml liquid and 20 g solid) and for 3 hours. In all leaching experiments, the stirrer speed was 500 rpm. According to the solubility of copper sulfate in water, the amount of copper sulfate production in the concentrate was measured by leaching in distilled water. Copper recovery was obtained by dividing the amount of copper dissolved onto the amount of initial copper in the concentrate.

DISCUSSION

The unreacted core model is one of the simplest and oldest models, which was first introduced by Yagi in 1955. In a series of non-porous solids reactions, a layer of solid product or even solid impurities encloses the unreacted solid core during the reaction [17]. In this model, it is assumed that the reaction initially begins with the outer shell of the object, and then the reaction zone moves into the object, and afterwards it left behind completely converted materials and also no-effect solid matters. Thus at any given moment there will be a core of unbou[illegible]d material in a solid matter which become smaller during the reaction [18].

In this model, the reaction rate can be controlled by the following three factors:

Diffusion to the gas film around the particle;

Diffusion to the ash layer of products;

Reaction at the interface of products and initial solid;

Unreacted core model can be used in solid-fluid reactions which have few porous particles.

Typically, decomposition reactions in solid state are described by the following single step kinetic equation:

$$dx/dt = k(T).f(x) \quad (1)$$

Where t indicates time, T temperature, x conversion rate and f(x) is the kinetic model. The integration of the above equation gives the integral relation of rate:

$$g(x) = kt \quad (2)$$

Table 1. Analysis of XRF chalcopyrite concentrate (%)

Cu	Fe	SiO2	CuO	Al2O3	S	Other compound
26.8	26.37	6.64	0.27	2.41	30.54	6.97

Table 2. Analysis of chalcopyrite concentrate mineralogy

Non-metallic minerals	Other metal minerals	Bornite Cu5FeS4	Covellite CuS	Chalcocite Cu2S	Pyrite FeS2	Chalcopyrite CuFeS2	Mineral type
15.53	1.2	0.48	1.3	0.5	12	69	Weight Percentage

If during the reaction, the volume and mass of the sample increases or remains constant, the unreacted core model is suitable for the process [18]. The kinetic equation of unreacted core model varies depending on the shape of particles. In addition, as mentioned in the previous section, the three factors of diffusion to the gas film around the particle, diffusion to the porous layer of reaction products and reaction at the interface between the raw materials and the products affect the reaction rate. Table 3 shows the different states of the unreacted core kinetic model. If the diffusion effect is minimized in the experiments, it is expected that the reaction is the only process controller factor, and other factors have been eliminated.

When the reaction is controller factor at the interface between the products and the initial solid, the following relation will be used [18]:

$$1-(1-x)^{1/3} = k_r.t \qquad (3)$$

where, x is the conversion rate, k_r indicates constant of the equation and t is the time.

If the diffusion is controller factor at the porous layer of solid products, the relation 3 will be used as follows [18]:

$$1-3(1-x)^{2/3}+2(1-x) = k_d.t \qquad (4)$$

where k_d is the equation constant.

Thermodynamics

The first step in examining the feasibility of thermal process of sulfate chalcopyrite oxidation is to investigate the thermodynamic equilibrium diagrams of iron and copper sulfides with respect to the variety of reactions and products of the roasting process. Studies on single sulfides, i.e. copper sulfide and iron sulfide, can help to understand the oxidation of their mixtures and also the oxidation of chalcopyrite [1]. By drawing the Kellogg Phase stability diagrams for Cu-S-O and Fe-S-O systems at temperatures of 500 to 600 ° C, it is observed that there is a range where we can produce simultaneously iron as a stable and insoluble oxide of hematite (Fe2O3) and also copper in the form of sulfate and oxy-sulfate which is soluble in water or dilute acid by controlling the roasting process (Fig. 1).

Table 3. Different states of the unreacted core kinetic model [17]

	Film Diffusion Controls	Ash Diffusion Controls	Reaction Controls
Flat plate $X = 1-\frac{1}{L}$ L= half thickness	$\frac{t}{\tau} = X$ $\tau = \frac{\rho_g L}{bK_g C_{Ag}}$	$\frac{t}{\tau} = X$ $\tau = \frac{\rho_g L^2}{2bD_e C_{Ag}}$	$\frac{t}{\tau} = X$ $\tau = \frac{\rho_g L}{bK^n C_{Ag}}$
Cylinder $X = 1-\left(\frac{r_c}{R}\right)^2$	$\frac{t}{\tau} = X$ $\tau = \frac{\rho_g R}{2bK_g C_{Ag}}$	$\frac{t}{\tau} = X + (1-X)\ln(1-X)$ $\tau = \frac{\rho_g R^2}{4bD_e C_{Ag}}$	$\frac{t}{\tau} = 1-(1-X)^{\frac{1}{2}}$ $\tau = \frac{\rho_g L}{bK^n C_{Ag}}$
Sphere $X = 1-\left(\frac{r_c}{R}\right)^3$	$\frac{t}{\tau} = X$ $\tau = \frac{\rho_g L}{3bK_g C_{Ag}}$	$\frac{t}{\tau} = 1-3(1-X)^{\frac{2}{3}}+2(1-X)$ $\tau = \frac{\rho_g R^2}{6bD_e C_{Ag}}$	$\frac{t}{\tau} = 1-(1-X)^{\frac{1}{3}}$ $\tau = \frac{\rho_g L}{bK^n C_{Ag}}$

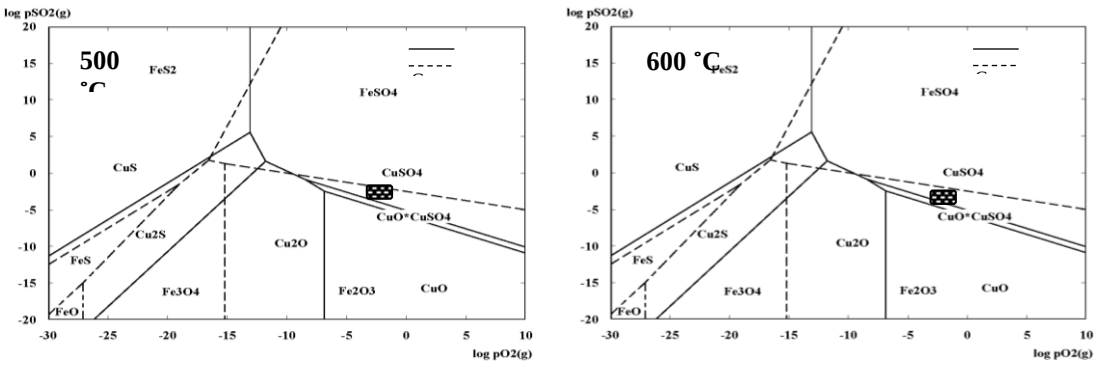

Figure 1. Kellogg phase stability diagrams for Cu-S-O and Fe-S-O systems at 500 and 600 ° C

The results of the thermal analysis of TGA and DSC for the chalcopyrite concentrate in the presence of the air atmosphere are shown in Figures 2 and 3, respectively. Comparative graphs show that the recorded curves are the same at different temperature increasing rates. As the temperature increases, the peaks are opened and move to higher temperatures in the both TGA and DSC diagrams. In the DSC diagram, the cause of overlapping the peaks at higher temperature rates is to increase the heating speed.

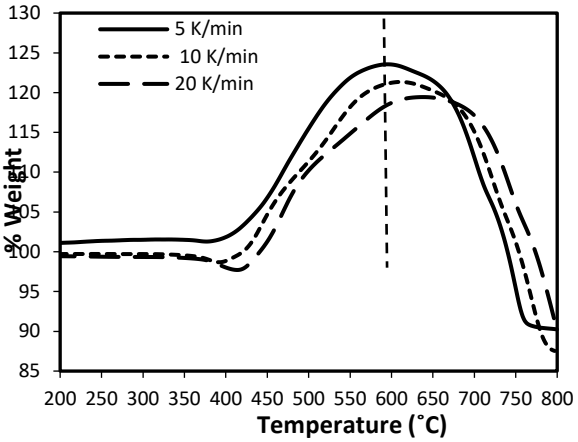

Fig. 2. TGA diagrams of the Sarcheshmeh chalcopyrite concentrate at three temperature increasing rates with air flow of 50 ml / min

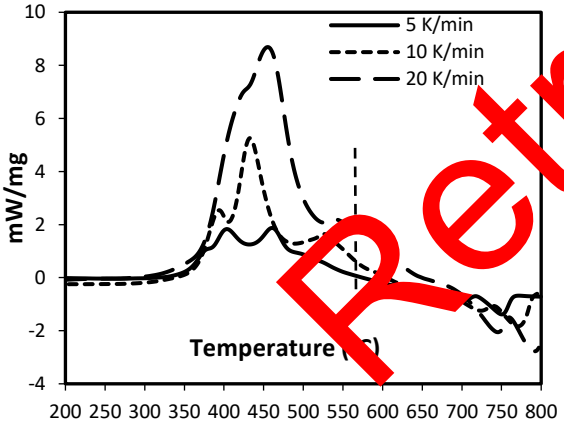

Fig. 3. DSC diagrams of the Sarcheshmeh chalcopyrite concentrate at three different temperature increasing rates with air flow of 50 ml / min.

The mechanism of roasting process

The mechanism of roasting process investigates to determine the steps and reactions which have taken place during the process. In this research, the mechanism of roasting process was studied both for temperature changes in constant time and also over time at constant temperature.

During the process of roasting, mass transfer occurs as the gas diffusion into the gas layer and the layer of porous solid (Fig. 4). Diffusion into the porous solid layer also involves gas diffusion into the porous layer of products and also the diffusion of iron solid cations and sulfur anions into the initial solid layer [19].

The mechanism of roasting process against temperature changes

The mechanism of roasting process against temperature changes was determined by analysing the TG-DSC curves and XRD analysis. The DSC curves include two parts: the first part is related to the process of sulfides oxidation at temperatures below 600 ° C and consists of three exothermic peaks, while the second part includes endothermic peaks which are related to the decomposition of copper sulfate and oxy-sulfate [20]. The two part in TG and DSC diagrams are split by dashed line.

The DSC curve, in Fig. 3, shows that chalcopyrite decomposition begins from the layers at the chalcopyrite surface, depending on the heating rate, at the temperature range of 340-370 ° C [7], so that by increasing energy levels, the decomposition at such temperature is evident without significant mass changes in the TG curve:

$$5Cu_2FeS_4 \rightarrow Cu_5FeS_4+4FeS+S_2 \quad (5)$$

In the following, an exothermic peak is observed immediately at a temperature range of 370-410 ˚C at the DSC diagram, which corresponds to the weight loss at the TG diagram. This change indicates intense oxidation at the inner layers of chalcopyrite, and also the simultaneous decomposition of the existing pyrite in sample as well as the production of magnetite [21, 7]:

$$2\ Cu_5FeS_4+O_2(g) \rightarrow 5Cu_2S+2FeS+SO_2 \quad (6)$$

$$2FeS_2+2O_2(g) \rightarrow 2FeS+2SO_2(g) \quad (7)$$

$$3FeS+5O_2 \rightarrow Fe_3O_4+3\ SO_2(g) \quad (8)$$

The produced pyrrhotite from the decomposition of chalcopyrite and pyrite is reacted with oxygen in the range of 420-500 ˚C, and the production of iron sulfate begins. In addition, the produced magnetite in the previous step is converted to hematite [21, 22], both of which increase mass in the sample:

$$FeS+2O_2(g) \rightarrow FeSO_4 \quad (9)$$

$$4\ Fe_3O_4+\ O_2 \rightarrow 6Fe_2O_3 \quad (10)$$

The sample mass increases by heating and a small exothermic peak is observed in the DSC diagram at different heating rate in the range of 500-540° C. At this stage of the roasting process, the copper sulfate and copper oxy-sulfate are produced [13, 20, 21], which causes a change in the intensity of mass increase in the sample:

$$Cu_2S+SO_2(g)+3O_2(g) \rightarrow 2CuSO_4 \quad (11)$$

$$2\ Cu_2S\ +5O_2(g) \rightarrow 2CuO.CuSO_4 \quad (12)$$

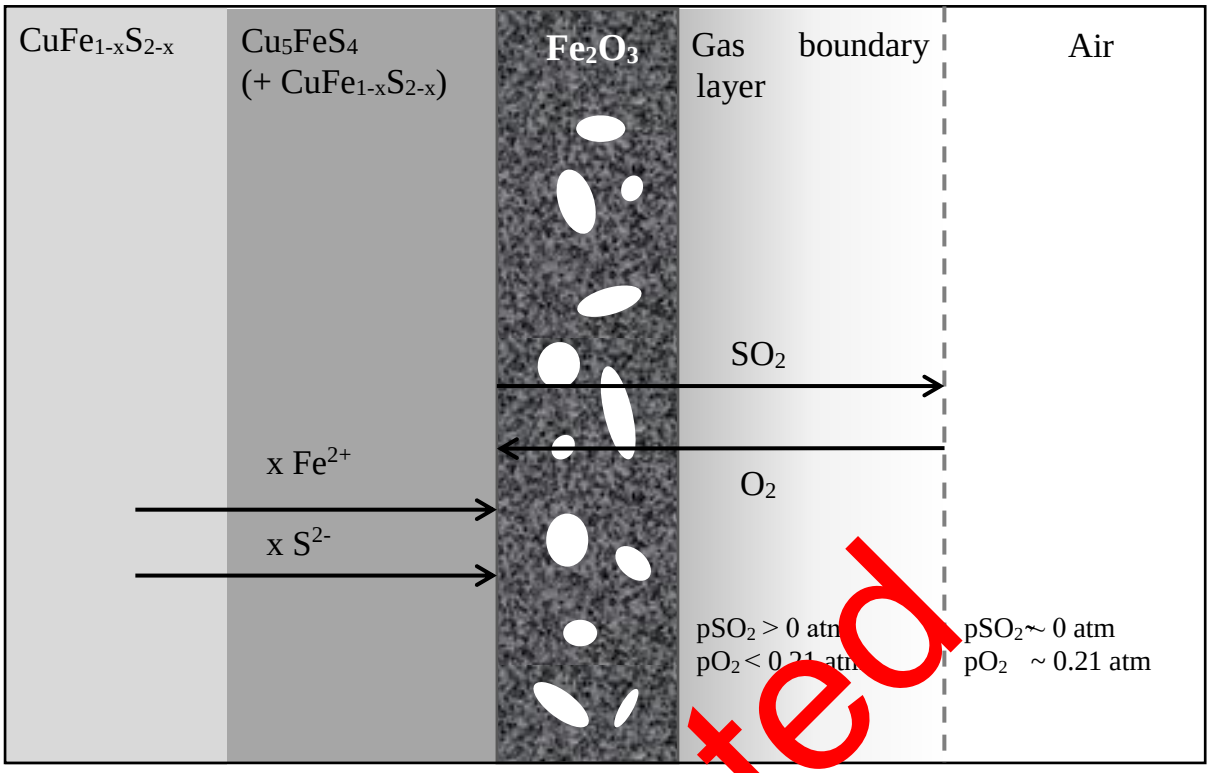

Fig. 4. Mass transfer mechanisms in the process of roasting

More intensity of mass increase observed in the DTG diagram which is the TG differential diagram in Fig. 5. Two peaks arise in the range of 400-550° due to a slope change in the TG diagram. The first peak is related to the start of production of iron sulfate and the second peak is belong to the beginning of the production of copper sulfate.

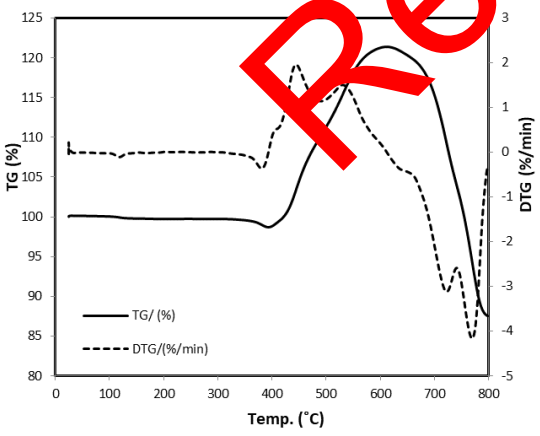

Fig. 5. TGA-DTG diagram of Sarcheshmeh concentrate at 10 ° K / min temperature increase rate

By increasing the temperature in the temperature range of 550-620 ˚C, the decomposition of iron sulfate begins [21, 22], which leads to a decrease in the slope of mass increase:

$$2FeSO_4 \rightarrow Fe_2O_3+SO_2+SO_3(g) \quad (13)$$

After temperature range of 620-650 ° C, copper sulfate and copper oxy-sulfate are converted into copper oxide:

$$CuSO_4 \rightarrow CuO+SO_3(g) \quad (14)$$

$$CuO.CuSO_4 \rightarrow 2CuO+SO_3(g) \quad (15)$$

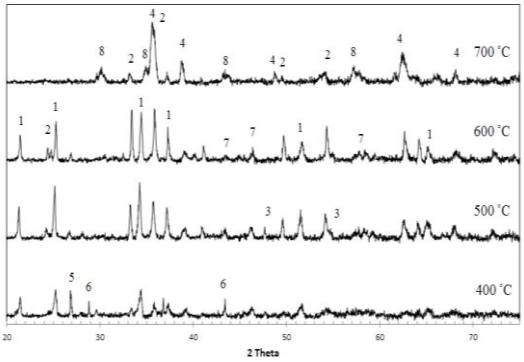

Figure 6. Comparative diagram of XRD analysis of the roasted concentrate at different temperatures for 30 minutes, 1) Chalcocyanite (CuSO4), 2) Hematite (Fe2O3), 3) Iron Sulfate (FeSO4), 4) Tenorite (CuO), 5) Bornite (Cu5FeS4), 6) Troilite (FeS), 7) Magnetite (Fe3O4), 8) Copper –iron oxide (CuFe2O4) (copper ferrite).

Figure 6 illustrates the XRD analysis diagram of the roasted samples at various temperatures. The presence of poor peaks of bornite at the temperature of 400 ° C confirms the transitory of this compound during the chalcopyrite roasting process. The iron sulfate peaks in the XRD diagram have been

generated at a temperature of 400°C and faded at 500 ° C. While copper sulfate peaks continue to appear at temperatures up to 600 ° C. In addition, the intensity of copper sulfate and iron oxide peaks is highest at 600 ° C. As a result, it can be claimed that As a result, it can be claimed that As a result, it can be claimed that sulfation and oxidation of iron sulfide occur before copper sulfides. At about 600 ° C, while almost all of the iron sulfate oxidized from the previous steps, the highest amount of copper sulfate is produced. At about 700 ° C, almost all of the iron and copper present in the concentrate are oxidized, and the oxide complex of iron and copper (CuFe2O4) is also observed.

For the state where the reaction is controller factor, mass transfer rate should be high in order to determine the reaction rate. In other words, it is necessary to remove the mass transfer resistance. The results of the experiments are presented in Figures 7 to 9, with the aim of investigating the proper conditions for the elimination or reduction of the gas diffusion factor effect in the concentrate bed.

As it can be seen, there is no change in the recovery rate from the height of 1 mm to the bottom (Fig. 7). As a result, the minimum proper substrate height, where gas penetration does not have an influence, was considered to be 1 mm. According to Fig. 8, particles below 325 mesh have the least effec of gas penetration on the recovery.

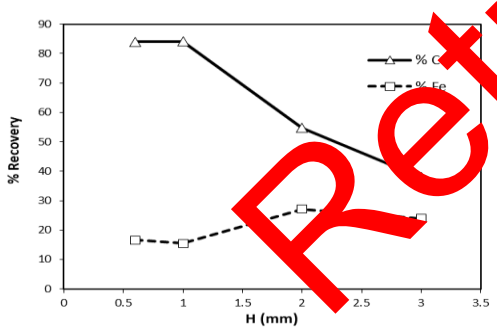

Figure 7. Effect of concentrate bed height on copper recovery; roasting the concentrate at 550 ° C and flow rate of 10 lit/min for 10 minutes.

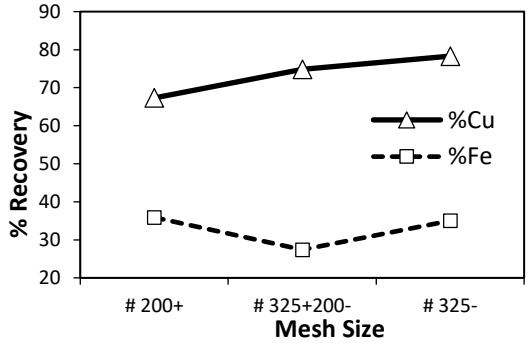

Figure 8: Effect of particle size on copper recovery; roasting the concentrate at 550 ° C and flow rate of 10 lit/min for 10 minutes

In addition, according to Figure 9, the effect of flow rate on diffusion in gas film around the particles is eliminated at flow rates above 8 lit/min. As a result, it can be claimed that the penetration process has the least effect on the rate of reaction in the conditions of the bed height for 1 mm, the particle size with -325 mesh and the air flow rate of 8 lit/min. In this case, the concentration of oxygen in the air was 2.5 times greater than the stoichiometry.

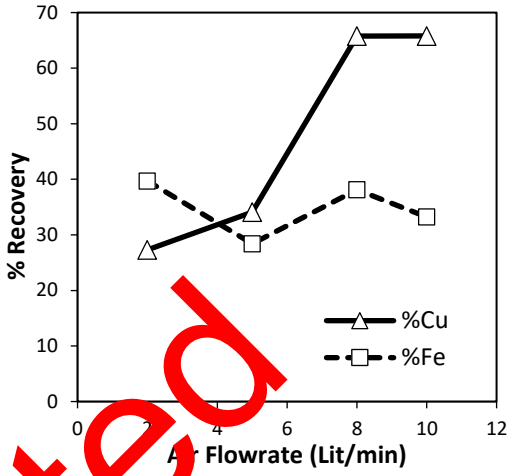

Figur Ef t r air flow rate on copper recovery; roa g at 50 ° C and particle size with -325 mesh.

tudy o the kinetics of copper sulfate production

After eliminating the influence of gas p tration, the rest of experiments were carried out nder conditions where the penetration has least influence on the reaction rate. A less than 5% error in the roasted concentrate mass in repeated experiments indicated that the experiments were repeatable. The leaching process of all the roasting products was carried out under the same conditions. The recovery results are shown relative to time and temperature in Figures 10, 11 and Table 4, respectively.

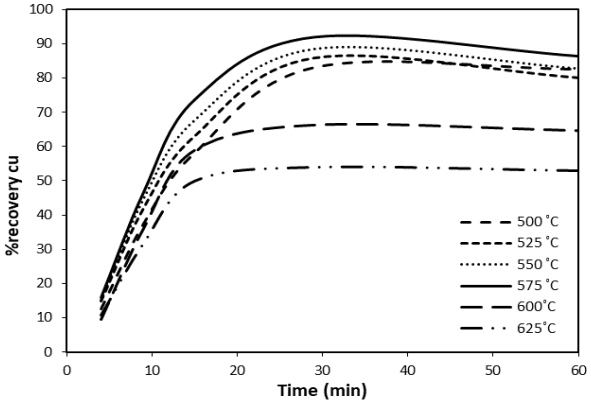

Figure 10. The percentage of dissolved copper in roasting products at constant temperature and different times in distilled water under conditions with minimum mass transfer resistance.

Table 4. The percentage of dissolved copper in roasting products at different temperature and times in distilled water under conditions with minimum mass transfer resistance

	500 ˚C	525 ˚C	550 ˚C	575 ˚C	600 ˚C	625 ˚C
5 min	12.57	14.35	15.23	15.82	10.30	11.47
10 min	37.57	42.1	44.82	46.70	43.20	34.12
15 min	58.25	67.13	67.80	73.7	64.50	55.81
30 min	83.17	85.86	88.60	91.84	70.15	58
60 min	82.64	80.10	82.84	86.30	69.50	53.64

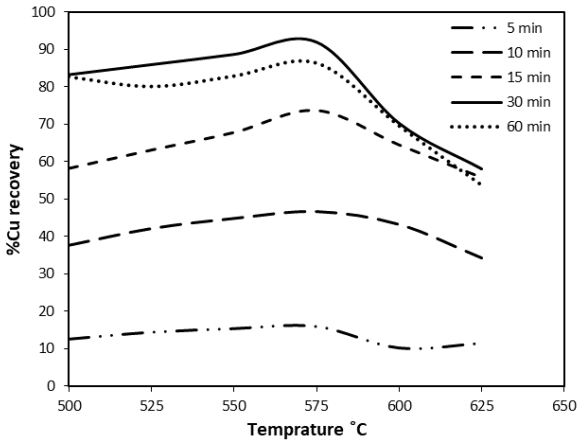

Figure 11. The percentage of dissolved copper in roasting products at constant time and in different temperature in distilled water under conditions with minimum mass transfer resistance.

In the conducted experiments, the rate of dissolution of iron in water leaching was very low. Figure 12 shows the recovery rate of iron at different temperatures over time. As it can be seen, at 575 °C, recovery of iron is less than 0.5% after 30 minutes.

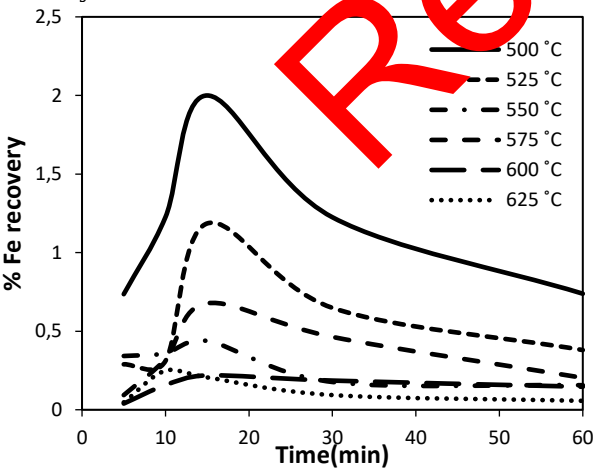

Figure 12. The percentage of dissolved iron concentrate at constant temperature and different times during roasting in conditions with minimum mass transfer resistance.

For calculating the kinetics of chalcopyrite sulfation reaction, it is first necessary to examine which penetration or reaction factor controls the reaction rate. We can determine the controlling factor of the reaction by plotting the conversion rate graph versus time and checking the correlation coefficient of data (R2). Also, the graph slope at each temperature is the apparent kinetic constant (kr, kd) at that temperature. Each of the equations with a higher correlation coefficient is the controller of the reaction. Figures 13 and 14 show the correlation coefficients of two models of penetration and reaction.

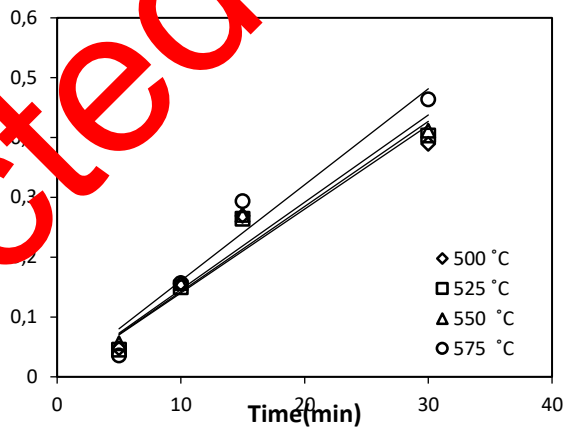

Figure 13. Chart of investigation for being controller of the reaction for chalcopyrite sulfation reaction in conditions with minimum mass transfer resistance.

Correlation coefficients and apparent kinetic constant for the mentioned models are presented in Table 5. As can be seen, the controller reaction model has greater correlation coefficients. As a result, it can be stated that the reaction is the controller of the reaction rate in the interface between the primary material and the products.

In addition, increasing the correlation coefficient in the penetration model with increasing temperature and simultaneously reducing the coefficient in the reaction model shows that with increasing temperature, the controlling factor for the penetration factor is greater and for the reaction agent is reduced. But at all temperatures, the reaction factor also has a higher correlation coefficient.

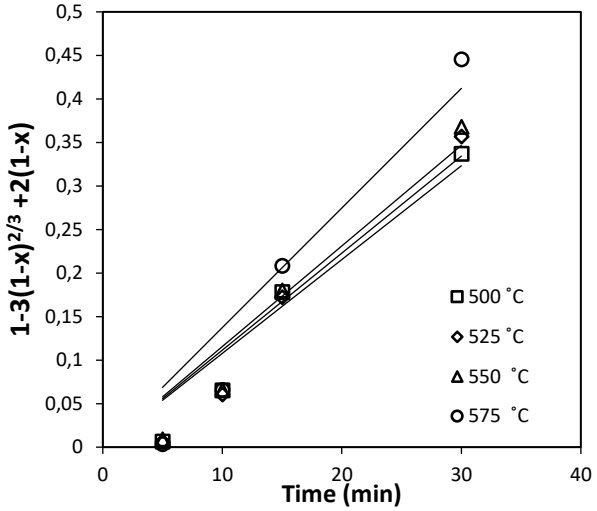

Figure 14. Chart of investigation for being controller of the diffusion of chalcopyrite sulfation reaction in conditions with minimum mass transfer resistance.

In addition, increasing the correlation coefficient in the penetration model with increasing temperature and simultaneously reducing the coefficient in the reaction model shows that with increasing temperature, the controlling factor for the penetration factor is greater and for the reaction agent is reduced. But at all temperatures, the reaction factor also has a higher correlation coefficient.

Correspondingly On the other hand, in previous studies [19], it has been pointed out that during the process of roasting, iron cations are released to the surface of the sulfidic nucleus in which it is oxidized and distributed as hematite Fe2O3. Simultaneously sulfuric anions react with oxygen to produce SO2 gas, which creates porosity in the hematite layer. As a result, the outer layer of hematite is not protective and it can be assumed that gas oxygen is released through this layer before it reacts at the sulfide / oxide interface.

Table 5. Correlation coefficients and apparent velocity constant of the reaction for different kinetic models

Temp. ˚C	1-(1-x)1/3		1-3(1-x)2/3+2(1-x)	
	kr	R2	kd	R2
500	0.0157	0.992	0.013	0.9123
525	0.0171	0.986	0.0148	0.9321
550	0.0185	0.979	0.167	0.939
575	0.0204	0.972	0.0195	0.9393

The activation energy of production reaction of copper sulfate was obtained by drawing the ln ks diagram versus 1/T and multiplying the slope in the general gas constant.

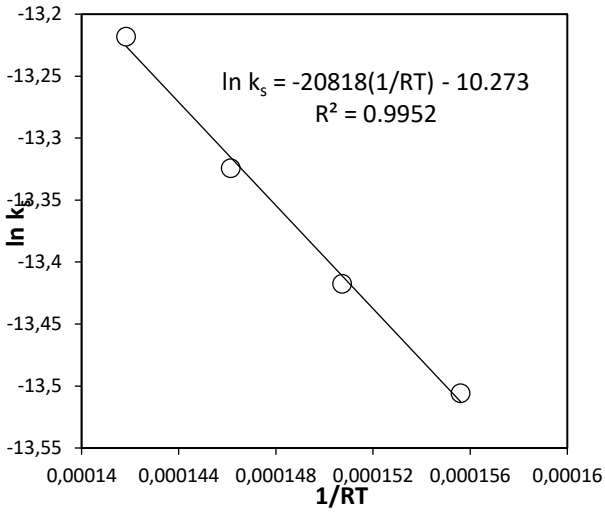

Fig. 15. Diagram of the activation energy determination of sulfation reaction of Sarcheshmeh copper concentrate

According to Fig. 15, the activation energy was obtained equal to 20.818 kJ/mol for sulfation reaction of chalcopyrite concentrate of Sarcheshmeh.

CONCLUSIONS

The mechanism of the complicated roasting process of chalcopyrite metal complex was determined by comparing the TG-DSC thermal analysis and XRD analysis. Studies have shown that the roasting process involves three steps of the decomposition of sulfides, the formation of sulfates and the production of metal oxides. The first two steps, which continue to a temperature of about 600°C, are accompanied by exothermic reactions that indicate the spontaneity of the process. At this temperature, copper and iron were observed as sulfate and oxide, respectively. The required heat for oxidation of iron is also provided by the energy released from other exothermic reactions. After this temperature, all the metal compounds were oxidized during the endothermic reactions.

The best conditions for producing the maximum copper sulfate from chalcopyrite was obtained at 575° C and for 30 minutes. In this condition, 92% of copper content was recovered as sulfate. However, only 0.5% of iron in concentrate was dissolved in water. The activation energy of copper sulfate production reaction was 20.818 kJ / mol.

REFERENCES

1. S. Prasad, B.D. Pandey, *Min. Eng.* **11**, 763(1998).
2. F. Habashi, Chalcopyrite; its Chemistory and Metallurgy, Mac-Graw Hill, (1987).
3. J.S. Greenough, The recovery of copper in sulfide ores by roasting, leaching, and electrolysis, Montana Tech Library, (1932).
4. M.G. Dorris, Oxidation of copper concentrate to

water-soluble copper, MSc Thesis, University of Arizona (1966).
5. C.J. Ferron, J.D. Cuyper, *Int.J.Miner. Process*. **35,** 225 (1992).
6. M. Yildirim, *Mineralogy and Mineral Beneficiation of Platinum-Group Elements*, **111,** 44 (2002).
7. P.C. Chaubal, H.Y. Sohn, *Metall. Trans. B*, **17**, 51 (1986).
8. L. S. Leung, *Metall. Trans.*, ***6B,*** 341 (1975).
9. E. Burger, D. Bourgarit, V. Frotte´, F. Pilon, *J. Therm. Anal. Calorim*, **103,** 249 (2011).
10. L.E. Sargsyan, A. M. Hovhannisyan, *Metall. Mining Ind.*, **2**, 225 (2010).
11. L.Y. Sargsyan, A.M. Hovhannisyan, *Russian J. Non-Ferrous Metals*, **51**, 386(2010).
12. R.I. Razouk, M.Y. Farah, R.S. Mikhall, G.A. Kolta, *J. Appl.Chem.* **12**, 190 (1962).
13. A.Mitovski, N. Strbac, I. Mihajlovic, M. Sokic, J. Stojanovic, *J Therm Anal Calorim*, **118,** 1277 (2014).
14. N.D. Ganguly, S.K. Mukherjee, *Chem. Eng. Sci.* **22,** 1091 (1967).
15. V.V.V.N.S. Ramakrishna Rao, K.P. Abraham, *Metall. Trans.*, **2,** 2463 (1971).
16. S. Parsad, B.D. Panday, S.K. Palit, *Metall. Mater. Trans.*, **27,** 465 (1996).
17. J. Szekely, J.W. Evans, H.Y. Sohn, Gas-Solid Reactions, Academic Press, (1976).
18. O. Levenspiel, Chemical Reaction Engineering. 2nd edition, Wiley, New York, (1972).
19. E. Burger, D. Bourgarit, V. Frotte, F. Pilon, *J. Therm. Anal. Calorim*, **103,** 249 (2011).
20. M. Sokic, I. Ilic, D. Zivkovic, N. Vuckovic, *METABK* **47,** 109 (2008).
21. Z.D. Zivkovic, N. Mitevska, V. Savovic, *Thermochim. Acta* **282/283** 121 (1996).
22. A. Mitovski, N. Štrabac, D. Manasijevic, M. Sokic', A. Dakovic, D. Zivcovic, L. Balanovic, *METABK*, **54,** 311 (2015).